

THREE-DIMENSIONAL TIME-DEPENDENT NEUTRON DIFFUSION SIMULATION USING AVERAGE CURRENT NODAL EXPANSION METHOD

by

Kambiz VALAVI, Ali PAZIRANDEH^{*}, and Gholamreza JAHANFARNIA

Department of Nuclear Engineering, Science and Research Branch,
Islamic Azad University, Punak, Tehran, Iran

Scientific paper

<https://doi.org/10.2298/NTRP2003189V>

In this work, the average current nodal expansion method was developed for the time-dependent neutronic simulation of transients in a nuclear reactor's core. For this purpose, an adopted iterative algorithm was proposed for solving the 3-D time-dependent neutron diffusion equation. In the average current nodal expansion method, the domain of the reactor core can be modeled by coarse meshes for neutronic calculation associated with reasonable precision of results. The discretization of time differential terms in the time-dependent equations was fulfilled, according to the implicit scheme. The proposed strategy was implemented in some kinetic problems including an infinite slab reactor, TWIGL 2-D seed-blanket reactor, and 3-D LMW LWR. At first, the steady-state solution was carried out for each test case, and then, the dynamic neutronic calculation was performed during the time for a specified transient scenario. Obtained results of static and dynamic solutions were verified in comparison with well-known references. Results can indicate the ability of the developed calculator to simulate transients in a nuclear reactor's core.

Key words: average current nodal expansion method, coarse meshes, diffusion equation, rectangular geometry, time-dependent calculation, transient simulation

INTRODUCTION

The design and safety assessment of new nuclear systems suggested for future improvement need accurate simulation of the behavior of neutron distribution during typical operational and accidental conditions [1]. Generally, two different strategies have been usually used for obtaining neutron flux distribution in a nuclear reactor core including the deterministic methods, *e. g.* the nodal method [2], and the probabilistic methods, *e. g.* the Monte Carlo method [3, 4]. As the numerical experiments noted in [5] and others, revealed insufficient accuracy of the *point-reactor* model for the analysis of large thermal light water reactors (LWR) [6], approximation strategies for solving the space-energy dependent neutron kinetics equations have been of interest in reactor physics ever since early 1960. However, one of the methods for predicting the accurate space-time distribution of neutrons in a nuclear reactor core is the implicit direct solution of time-dependent multi-group neutron diffusion equation.

For solving the 3-D kinetics equation, techniques must be considered for space and time

discretization. Up to now, several methods have been developed and proposed for the spatial discretization of the neutron diffusion equation such as finite difference, finite element, and nodal methods. The space discretization technique is utilized for calculating the eigenvalue and also the flux distribution across the reactor core. In nodal methods, coarse meshes can be employed according to sizes of a fuel assembly (FA) accompanied by retaining tolerable accuracy. Among the well-known nodal methods, the analytical nodal method (ANM) [7] and the nodal expansion method (NEM) [8], should be mentioned. In the ANM, the neutron diffusion equation is solved analytically but in the NEM, this equation is solved by defining a polynomial expansion the coefficients of which are determined in terms of nodal parameters for each node and energy group. Recently, a steady-state calculation package has been developed in order to evaluate the accuracy of NEM sub-methods for the 3-D rectangular geometry [9]. In addition, results of a static simulator for the 3-D hexagonal geometry using the average current nodal expansion method (ACNEM) have also been reported [10].

Various strategies have been applied for the time discretization of the time-dependent neutron diffusion

^{*} Corresponding author; e-mail: paziran@ut.ac.ir

equation. Standard methods employ backward difference formulas [11]. These methods require solving of a large system of linear equations at each time step. For solving these systems, preconditioned iterative methods are utilized [12]. Other types of methods such as modal approaches [13], and the quasi-static method [14], have also been implemented in the nuclear engineering field [15].

For the purpose of this paper, a space-time simulator was developed for analyzing the dynamical neutronic behavior of a nuclear reactor core, when a specific transient scheme was considered. In this way, a sub-method from the zeroth order NEM family, *i. e.* the average current approach, was used for the coarse mesh discretization of space in the coupled 3-D multi-group diffusion and the delayed neutron emitter concentration equations. The implicit backward Euler approach was also employed as the time discretization technique of noted time-dependent equations. In this work, an adapted iterative algorithm was proposed for solving the space-time multi-group neutron diffusion equation coupled with precursor equations. In this case, a novel iterative algorithm which had been proposed earlier for only steady-state calculations of ACNEM [9, 16], was developed for resolving the time-dependent neutron diffusion equations. As in each time-step of a transient simulation, using the fully implicit scheme, numerous time-consuming calculations should be performed and the computational cost of space-time solutions is really huge, the basic version of ACNEM, *i. e.* the zeroth order solution, was selected and applied in this work for discretizing the geometry domain. For evaluating the proposed methodology, three popular transient benchmarks were investigated and the obtained results were compared with the verified references. Results showed that the developed time-dependent ACNEM using the proposed iterative algorithm worked sufficiently well in simulating transient problems by coarse meshes.

AVERAGE CURRENT NODAL EXPANSION METHOD

Static calculation

The average current method [8, 17], is a NEM which is used for the steady-state neutronic calculation of a nuclear reactor core. Lately, this method has been discussed in some papers such as [9, 16]. That is why this methodology for 2-D diffusion equation is briefly presented in this paper.

The static multi-group neutron diffusion equation is given by the following

$$\begin{aligned}
 & \cdot J_g(\bar{r}) \quad r_g \phi_g(\bar{r}) \quad \frac{G}{g} \quad \frac{1}{g} \quad gg \phi_g(\bar{r}) \\
 & \frac{\chi_g}{k_{eff}} \quad \frac{G}{g} \quad \frac{1}{g} \quad \nu \quad f_g \phi_g(\bar{r}) \quad 0, \quad g = 1, 2, \dots, G \quad (1)
 \end{aligned}$$

where J_g and ϕ_g are the neutron current and flux in the location of \bar{r} , respectively.

In the ACNEM, a polynomial expansion is considered for the flux distribution in each node and energy group. For the zeroth order of ACNEM, the degree of this polynomial expansion is two which is defined generally by the following

$$\begin{aligned}
 \phi_g(x, y) &= A_g h_0 + a_{gx} h_1(x) + b_{gx} h_2(x) \\
 &+ a_{gy} h_1(y) + b_{gy} h_2(y) + c_g h_1(x) h_1(y) \quad (2)
 \end{aligned}$$

where $h_0 = 1, h_1(u) = u, h_2(u) = u^2 - \frac{1}{12}$, and $u = x, y$

By imposing the conditions of

$$\begin{aligned}
 & \frac{1}{V^m} \int_{\Pi^m} \phi_g d\Pi^m = \Phi_g^m \\
 & \frac{1}{A_{us}^m} \int_{\Gamma_{us}^m} \phi_g d\Gamma_{us}^m = \Psi_{gus}^m \quad (3)
 \end{aligned}$$

where Γ_{us}^m is the left ($s = l$)/right ($s = r$) u -surface of node Π^m , A_{us}^m is the area of Γ_{us}^m , Ψ_{gus}^m is the average flux for group g at Γ_{us}^m , and Φ_g^m is the average flux for group g in Π^m and by solving eq. (3), the expansion coefficients of A_g, a_{gu} , and b_{gu} noted in eq. (2) are obtained as the following relation

$$\begin{aligned}
 & A_g \quad \Phi_g^m \\
 & a_{gu} \quad \Psi_{gur}^m \quad \Psi_{gul}^m \\
 & b_{gu} \quad 3(\Psi_{gur}^m \quad \Psi_{gul}^m \quad 2\Phi_g^m) \quad (4)
 \end{aligned}$$

Therefore, if Φ_g^m and Ψ_{gus}^m parameters are specified, eq. (2) is determined for each node and energy group. For this purpose, eq. (1) is integrated first over each node m and in the following the 2-D multi-group neutron continuity equation is derived as

$$\begin{aligned}
 & \frac{1}{h_u^m} \{ j_{gus}^m \quad j_{gus}^m \} \quad \frac{m}{rg} \Phi_g^m \\
 & \frac{G}{g} \quad \frac{1}{g} \quad \frac{m}{gg} \Phi_g^m \quad \frac{\chi_g}{k_{eff}} \quad \frac{G}{g} \quad \frac{1}{g} \quad \nu \quad \frac{m}{fg} \Phi_g^m, \quad (5) \\
 & m = 1, 2, \dots, M, \quad g = 1, 2, \dots, G, \quad u = x, y
 \end{aligned}$$

where j_{gus}^m, j_{gus}^m are average outgoing (+) and incoming (-) partial currents for group g at Γ_{us}^m , respectively, and h_u^m is the thickness of node Π^m for the u direction.

For resolving eq. (5), additional relations are required in order to calculate the average surface partial currents (j_{gus}^m, j_{gus}^m). For this purpose, the Flick's law is applied by employing the defined neutron flux, eq. (2), for each node and energy group. Hence for the surface of Γ_{ul}^m , eq. (6) is obtained as follows

$$\begin{aligned}
 & j_{gul}^m \quad j_{gul}^m \quad \int_{\Gamma_{ul}^m} D_g \phi_g e_{ul}^m d\Gamma_{ul}^m \\
 & \frac{D_g^m}{h_u^m} (2\Psi_{gur}^m \quad 4\Psi_{gul}^m \quad 6\Phi_g^m) \quad (6)
 \end{aligned}$$

where e_{ul}^m is a unit vector in the direction of the outward normal to Γ_{ul}^m . Also by using the approximation of the following

$$\Psi_{gus}^m = 2(j_{gus}^m - j_{gus}^m), \quad s = 1, r, \quad u = x, y \quad (7)$$

For both surfaces of Γ_{ul}^m and Γ_{ur}^m , at last, a set of equations is arrived at in which the outgoing currents are related to the incoming currents and the average flux in each node. So the interface current equations are given by the following

$$\begin{pmatrix} j_{gul}^m \\ j_{gwr}^m \end{pmatrix} = \begin{pmatrix} A_{gu}^m & B_{gu}^m & C_{gu}^m \\ A_{gu}^m & C_{gu}^m & B_{gu}^m \end{pmatrix} \begin{pmatrix} \Phi_g^m \\ j_{gul}^m \\ j_{gur}^m \end{pmatrix}, \quad (8)$$

$$m = 1, 2, \dots, M, \quad g = 1, 2, \dots, G, \quad u = x, y$$

where A_{gu}^m, B_{gu}^m and C_{gu}^m are specified in terms of D_g^m and h_u^m for the node m and energy group g .

Now if the outgoing currents are eliminated from eq. (5) by using eq. (8), the final form of nodal balance equation is as follows

$$\begin{aligned} & u = x, y \quad 2 \frac{A_{gu}^m}{h_u^m} \sum_{rg}^m \Phi_g^m - \frac{G}{g} \frac{1}{g} \Phi_g^m \\ & \frac{\chi_g}{k_{\text{eff}}} \frac{G}{g=1} \nu \frac{1}{f_g} \Phi_g^m - \frac{u = x, y}{s = 1, r} \frac{1}{h_u^m} (1 - B_{gu}^m - C_{gu}^m) j_{gus}^m, \quad (9) \\ & m = 1, 2, \dots, M, \quad g = 1, 2, \dots, G, \quad u = x, y \end{aligned}$$

However, for obtaining the required unknown nodal parameters, eqs. (11) and (12) are solved accompanied by utilizing the continuity of interface currents for neighbor nodes and boundary conditions for exterior nodes. For a boundary surface, Γ_{us}^m , the following relation is used

$$j_{gus}^m = \frac{1}{1 - 2\lambda_{gus}^m} j_{gus}^m \quad (10)$$

where for reflecting and zero-flux boundary conditions, the λ_{gus}^m is considered by 0 and 10^{10} , respectively.

The power method is also applied for updating the multiplication factor, k_{eff} . The aforementioned procedure is illustrated in fig. 1 as a novel adopted iterative algorithm for static problems [9].

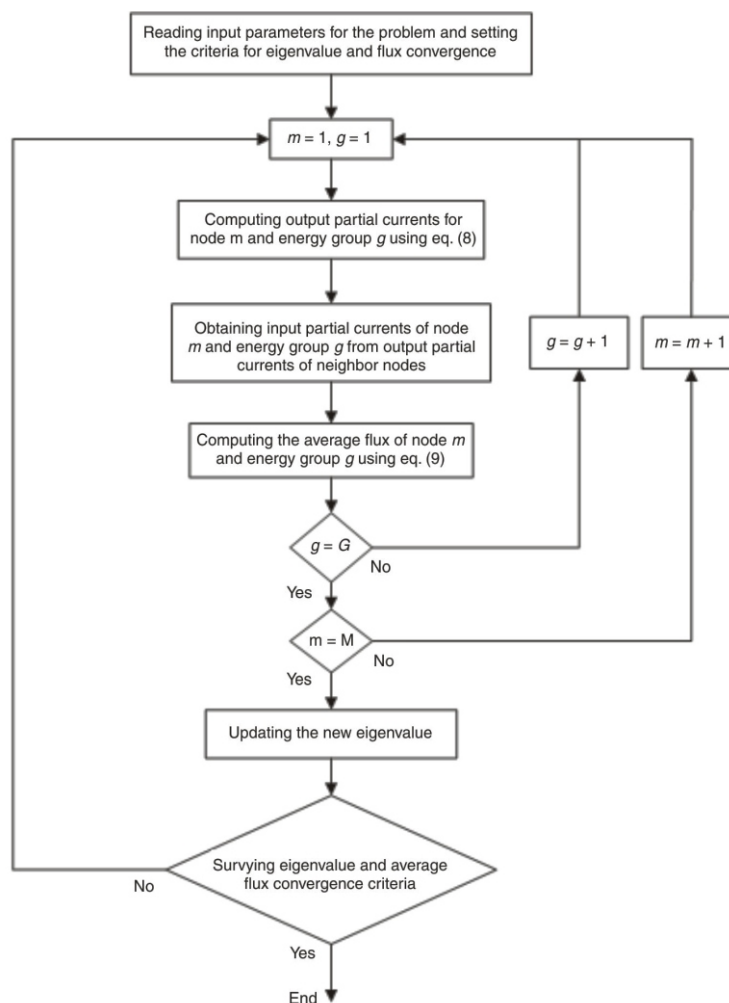


Figure 1. The flowchart of proposed adopted iterative algorithm for static calculation using ACNEM

For solving the system of nodal equations in ACNEM, the formal Gauss Seidel algorithm can be used. But, in some situations, the solution using the noted algorithm is diverged. According to [16], a novel adopted iterative algorithm has been proposed for overbearing the divergence problem of static solution using ACNEM. In the formal Gauss Seidel approach, the nodal parameters are updated and inner iterations are repeated until the solution is converged and then, the multiplication factor, k_{eff} is updated. But, for the proposed approach, in each inner iteration of Gauss Seidel algorithm, the multiplication factor k_{eff} is updated by using last nodal parameters and then the subsequent inner iteration is performed by using the new k_{eff} . By employing this iterative approach, the divergence of the solution does not appear [16]. In this paper, the noted novel methodology was used and extended for treating the time-dependent neutron diffusion equations.

Dynamic calculation

In this section, the steady-state strategy mentioned in the previous section is extended and developed for solving the time-dependent diffusion equations, in order to simulate transient neutronic scenarios in the reactor core.

The time-dependent form of eq. (1) is considered by [18]

$$\frac{1}{v_g} \frac{\partial}{\partial t} \phi_g(\bar{r}, t) = J_g(\bar{r}, t) - r_g(\bar{r}, t) \phi_g(\bar{r}, t) - \sum_{g=1}^G \sum_{g=1}^G (\bar{r}, t) \phi_g(\bar{r}, t) - \sum_{g=1}^G (1 - \beta) \frac{\chi_{pg}}{k_{\text{eff}}} v_{fg}(\bar{r}, t) \phi_g(\bar{r}, t) - \sum_{i=1}^I \lambda_i \chi_{dg}^i c_i(\bar{r}, t), \quad g = 1, 2, \dots, G \quad (11)$$

where v_g is the neutron velocity for energy group g , β is the total fraction of delayed neutrons, χ_{pg} and χ_{dg} are the emission spectrum of prompt and delayed neutrons for group g , respectively, λ_i is the decay constant of the i^{th} delayed neutron family, and c_i is the concentration of the i^{th} delayed neutron family.

Moreover, the concentrations of delayed neutron emitters, $c_i(\bar{r}, t)$, satisfy the following time-dependent balance equations, which are named the precursor equations, *i. e.*

$$\frac{\partial}{\partial t} c_i(\bar{r}, t) = \frac{1}{k_{\text{eff}}} \beta_i \sum_{g=1}^G v_{fg}(\bar{r}, t) \phi_g(\bar{r}, t) - \lambda_i c_i(\bar{r}, t), \quad i = 1, 2, \dots, I \quad (12)$$

where β_i is the delayed neutron fraction of the i^{th} delayed neutron family and I is the number of delayed neutron families [18].

If eq. (11) is integrated over the volume of node m , term by term, the following equation is derived for time t and energy group g

$$\frac{1}{v_g} \frac{d}{dt} \Phi_g^m(t) = \sum_{s=1, r}^{u, x, y} \frac{1}{h_u^m} \{j_{gus}^m(t) - j_{gus}^m(t)\} - r_g^m(t) \Phi_g^m(t) - \sum_{g=1}^G \sum_{g=1}^G (\Phi_g^m(t)) - \sum_{g=1}^G (1 - \beta) \frac{\chi_{pg}}{k_{\text{eff}}} v_{fg}^m(t) \Phi_g^m(t) - \sum_{i=1}^I \lambda_i \chi_{dg}^i c_i^m(t), \quad g = 1, 2, \dots, G \quad (13)$$

In the same way, eq. (12) for the precursor concentrations in the node-wise integrated form resulted as

$$\frac{d}{dt} c_i^m(t) = \sum_{g=1}^G \beta_i v_{fg}^m(t) \Phi_g^m(t) - \lambda_i c_i^m(t), \quad i = 1, 2, \dots, I \quad (14)$$

Similar to static treatment, an additional set of equations is needed for solving time-dependent coupled eqs. (13) and (14), *i. e.*

$$\begin{matrix} j_{gul}^m(t) & A_{gu}^m(t) & B_{gu}^m(t) & C_{gu}^m(t) & \Phi_g^m(t) \\ j_{gur}^m(t) & A_{gu}^m(t) & C_{gu}^m(t) & B_{gu}^m(t) & j_{gul}^m(t) \\ & & & & j_{gur}^m(t) \end{matrix} \quad (15)$$

$m = 1, 2, \dots, M, \quad g = 1, 2, \dots, G, \quad u = x, y$

Now by eliminating the outgoing currents from eq. (13) using eq. (15), we have the following

$$\frac{1}{v_g} \frac{d}{dt} \Phi_g^m(t) = \sum_{s=1, r}^{u, x, y} \frac{1}{h_u^m} [1 - B_{gu}^m(t) - C_{gu}^m(t)] j_{gus}^m(t) - r_g^m(t) \Phi_g^m(t) - \sum_{g=1}^G \sum_{g=1}^G (\Phi_g^m(t)) - \sum_{g=1}^G (1 - \beta) \frac{\chi_{pg}}{k_{\text{eff}}} v_{fg}^m(t) \Phi_g^m(t) - \sum_{i=1}^I \lambda_i \chi_{dg}^i c_i^m(t), \quad m = 1, 2, \dots, M, \quad g = 1, 2, \dots, G \quad (16)$$

For discretization of the time differential terms of eqs. (14) and (16), the implicit approach using the backward Euler method was utilized for the time t by the following

$$\frac{d}{dt} \Phi_g^m(t) = \frac{\Phi_g^m(t) - \Phi_g^m(t - \Delta t)}{\Delta t} = F^t - L^t \quad (17)$$

$$\frac{d}{dt} c_i^m(t) = \frac{c_i^m(t) - c_i^m(t - \Delta t)}{\Delta t} = F^t - L^t \quad (18)$$

where Δt is the time step, the operators F and L are the neutron production and consumption terms of eq. (16)

and also F and L are the precursors of production and consumption terms of eq. (14), respectively.

Ultimately, the final form of time-dependent multi-group neutron balance equation, eq. (16), using eq. (17), is obtained as follows

$$\begin{aligned} \Phi_g^m(t) &= \Phi_g^m(t - \Delta t) + v_{g,1} \Delta t \left[\sum_{s=1}^G \sum_{r=1}^M \frac{1}{h_{us}^m} [1 - \beta_{gs}] B_{gu}^m(t) \right. \\ &+ \sum_{s=1}^G \sum_{r=1}^M \frac{A_{gu}^m(t)}{h_{us}^m} \lambda_{rg}^m(t) \Phi_g^m(t) \\ &+ \sum_{s=1}^G \sum_{r=1}^M \frac{v_{gs}}{k_{eff}} (1 - \beta_{gs}) \frac{\chi_{pg}}{k_{eff}} v_{fg}^m(t) \Phi_g^m(t) \\ &\left. + \sum_{i=1}^I \lambda_i \chi_{dg}^i c_i^m(t) \right], \end{aligned} \quad (19)$$

$m = 1, 2, \dots, M, \quad g = 1, 2, \dots, G$

For the time-dependent equations of delayed neutron emitter concentration, the final form of eq. (14) is obtained by using eq. (18) in the following relation

$$\begin{aligned} c_i^m(t) &= \frac{1}{1 - \lambda_i \Delta t} \\ c_i^m(t - \Delta t) &+ \Delta t \frac{1}{k_{eff}} \beta_{i,g} v_{fg}^m(t) \Phi_g^m(t), \end{aligned} \quad (20)$$

$m = 1, 2, \dots, M, \quad i = 1, 2, \dots, I$

For solving the coupled time-dependent eqs. (19) and (20), an adopted iterative strategy for the time-dependent calculation of ACNEM was developed which is demonstrated in fig. 2. In this approach, the critical parameters of neutron balance equation were first computed including average fluxes and sur-

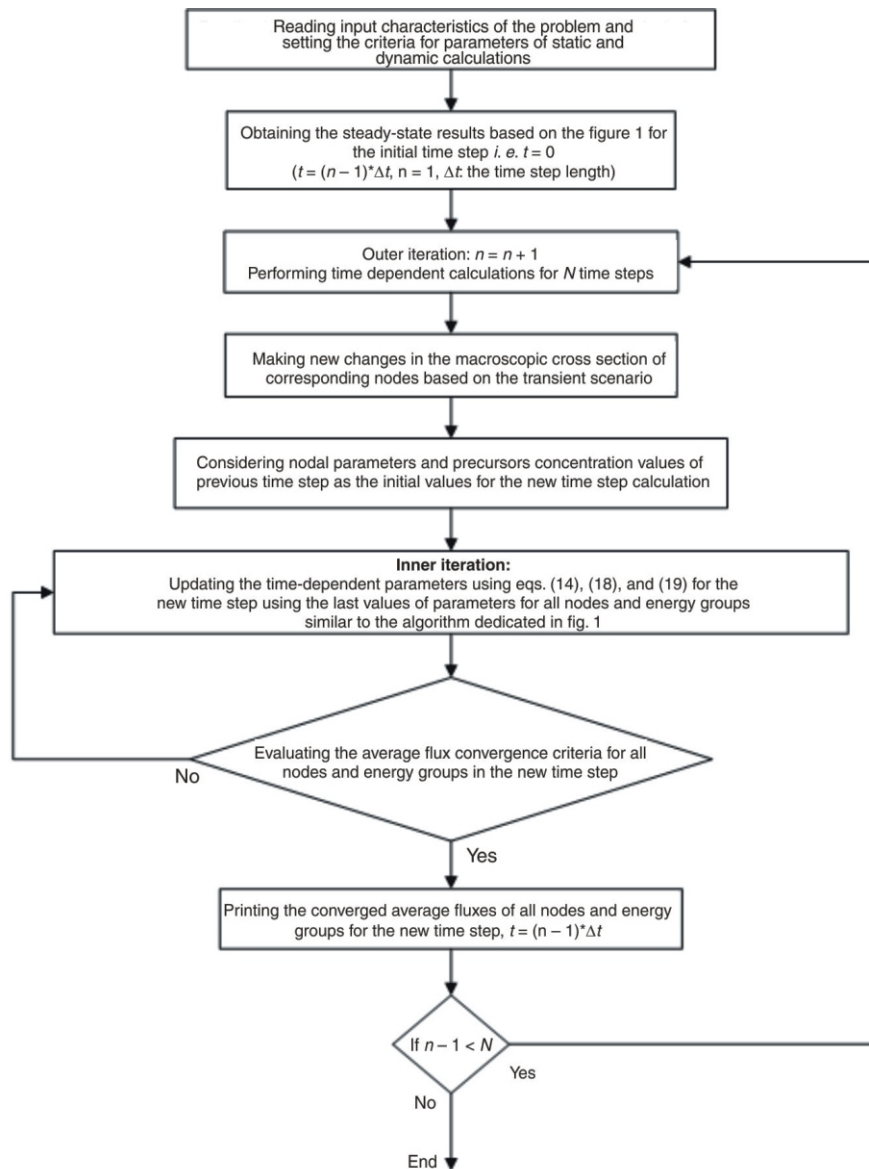


Figure 2. The flowchart of proposed adopted iterative algorithm for dynamic calculation using ACNEM

face partial currents of all nodes and energy groups and also precursor's concentrations of all nodes. Then time-dependent calculations were done for N time steps of Δt seconds using required parameters achieved in the previous time step. In each time step, variations of cross sections are performed, according to the defined transient scheme in the reactor core. In addition, an inner iteration was implemented for converging the average fluxes of all nodes and energy groups similar to the algorithm used in the static calculation presented in fig. 1. In this inner iteration, parameters of the previous time step including the average fluxes and currents are used as the initial values for the current time step and computations were repeated employing eqs. (15), (19), and (20) by using the nodal parameters of last inner iteration. This process was continued for the current time step until all of acquired average fluxes converged. Afterward, calculations were started for the subsequent time step until the end time of dynamic scenario was finally reached.

NUMERICAL RESULTS

In this section, the results of three transient test cases including an infinite slab reactor, TWIGL-2-D seed-blanket reactor and 3-D LMW LWR are given for both static and dynamic calculations, and also their results are compared with the reported results in references.

Problem 1: An infinite slab reactor

For the first test case, a 1-D reactor was introduced and investigated. This reactor was divided into three regions. Two outer regions (1 and 3) had 40 cm stick and also the size of central region (2) was 160 cm. For this problem, the boundary condition was the zero flux. The two-group constants of the problem are presented in tab. 1. In addition, parameters of six groups of delayed neutrons for the transient analysis of infi-

Table 1. Cross-sections of the infinite slab reactor model

Region	Group [g]	D_g [cm]	Σ_{ag} [cm ⁻¹]	$\nu\Sigma_{fg}$ [cm ⁻¹]	Σ_{1-2} [cm ⁻¹]
1,3	1	1.50	0.011	0.010	0.015
	2	0.50	0.180	0.200	
2	1	1.00	0.010	0.005	0.010
	2	0.50	0.080	0.099	

$$v_1 = 1.0 \cdot 10^7 \text{ cms}^{-1}, v_2 = 3.0 \cdot 10^5 \text{ cms}^{-1}$$

Table 2. Parameters of delayed neutrons for the infinite slab reactor model

Parameter	$d = 1$	$d = 2$	$d = 3$	$d = 4$	$d = 5$	$d = 6$
β_d	0.00025	0.00164	0.00147	0.00296	0.00086	0.00032
λ_d	0.0124	0.0305	0.1110	0.3010	1.1400	3.0100

nite slab reactor model are shown in tab. 2 [19]. This example was solved by 24 coarse nodes having the size of 10 cm. The effective multiplication factor and relative regional powers of the static calculation were compared with the reference in tab. 3. The benchmark problem book [20], reported the reference solution which has been obtained by a finite-difference code with 2 cm meshes. According to relative errors given in tab. 3, static results indicated an accurate solution in respect to the reference.

For the dynamic calculation, the transient scheme was a linear increment of 3 % in the thermal absorption cross-section for region 1 in 1.0 second. The dynamic solution was performed by using the developed time-dependent ACNEM and considering the time step of 0.01 second. As for fig. 2, the time-dependent calculation has been done step by step for 2 seconds with 200 time steps. The obtained relative total powers are represented in tab. 4 for selected times and compared for some times with the reference [20]. The minor diversity of results in comparison with those in the reference can be seen in tab. 4. The diagrams of obtained relative total powers and the reference along the time are also illustrated in fig. 3.

For this test case, a sensitivity analysis was made for time step and mesh size parameters. Table 5 gives some results for various mesh sizes including the CPU time and the average and maximum relative errors of time-dependent total powers which were compared with the reference. Similarly, the CPU time and the average and maximum relative errors of noted powers for various time steps are also presented in tab. 6. Using the developed procedure, it is found that no divergence appeared for various mesh sizes and time steps in transient calculations. Tables 5 and 6 indicate that when the mesh sizes and time steps are decreased and consequently, the CPU time is increased, the accuracy of time-dependent powers obtained by ACNEM has not changed considerably. Thus, the calculations for the following problems were done for coarse meshes and a time step.

Table 3. Results of the static calculation for infinite slab reactor model

Parameter	ACNEM	Reference	Relative error [%]
k_{eff}	0.90090	0.90155	-0.07
Relative power of reg.1 ^a	0.829	0.837	-0.91
Relative power of reg.2 ^a	1.341	1.326	1.15
Relative power of reg.3 ^a	0.829	0.837	-0.91

^a Relative power (normalized to the average value of regional powers)

Table 4. Relative total power vs. time for infinite slab reactor model

Time [s]	ACNEM ^a	Reference	Relative error [%]
0.00	1.000	1.000	—
0.10	0.931	0.930	0.087
0.20	0.875	0.873	0.209
0.30	0.830	—	—
0.40	0.793	—	—
0.50	0.762	0.760	0.235
0.60	0.735	—	—
0.70	0.713	—	—
0.80	0.693	—	—
0.90	0.676	—	—
1.00	0.661	0.659	0.266
1.50	0.645	0.643	0.321
2.00	0.632	0.631	0.224

^a Mesh size: 10 cm, time step length: 10⁻² s

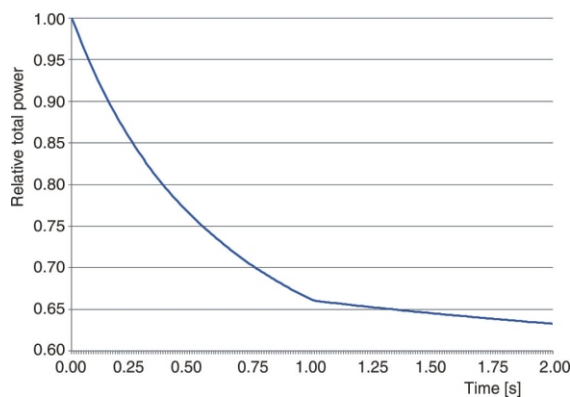


Figure 3. Relative total power vs. time for the infinite slab reactor

Table 5. Results of various mesh sizes for infinite slab reactor model

Mesh size [cm]	CPU time [s] ^a	Average relative error, [%]	Maximal relative error, [%]
2.5	410	0.10	0.19
5	70	0.12	0.21
10	12	0.22	0.32

^awith laptop corei5, 2.4 HGz

Table 6. Results of various time steps for infinite slab reactor model

Time step [s]	CPU time [s] ^a	Average relative error, [%]	Maximal relative error, [%]
10 ⁻¹	3	0.23	0.30
10 ⁻²	12	0.22	0.32
10 ⁻³	60	0.23	0.31

^awith laptop corei5, 2.4 HGz

Problem 2: TWIGL seed-blanket reactor

This test case is a 2-D model of a 160 cm square un-reflected seed-blanket reactor. The problem was defined with two neutron energy groups and eighth symmetry of the core. At first, transient solutions were obtained by [21] and surveyed in documents such as [7, 19]. For this transient problem, all of required neutronic data are given in tab. 7 and the geometry is also exhibited in fig. 4 [19].

Table 7. Characteristics of TWIGL SEED-BLANKET-2-D reactor problem

Region	Group, g	D _g [cm]	Σ _{ag} [cm ⁻¹]	νΣ _{f_g} [cm ⁻¹]	Σ _{1→2} [cm ⁻¹]
1,3	1	1.4	0.01	0.007	0.01
	2	0.4	0.15	0.2	
2	1	1.3	0.008	0.003	0.01
	2	0.5	0.05	0.06	

v₁ = 1.0 10⁷ cms⁻¹, v₂ = 2.0 10⁵ cms⁻¹, β = 0.0075, λ = 0.08

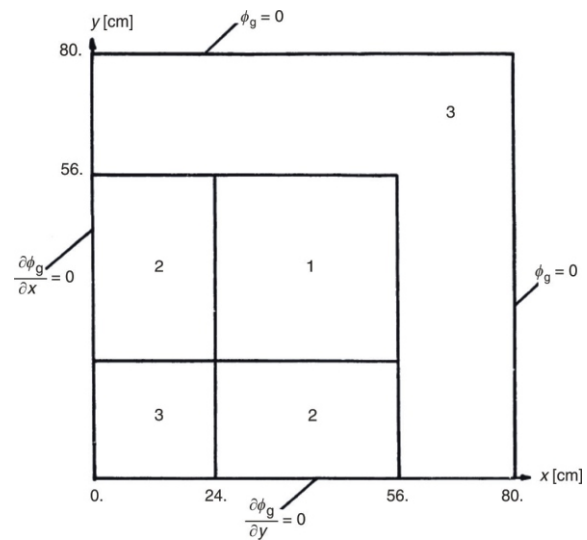


Figure 4. Quadrant of TWIGL seed-blanket reactor geometry

The static solution of ACNEM was fulfilled by using 8 cm × 8 cm meshes and its results and relative errors in comparison to reference are represented in tab. 8. The reference is the second order calculation of ACNEM reported in [19]. The comparison of data noted in tab. 8, confirms the true static solution of applied ACNEM.

For this problem, two transients were initiated in region 1 by decreasing the thermal absorption cross section including the step perturbation as the following

$$\Delta a_2 = -0.0035 \text{ cm}^{-1}, t = 0 \quad (21)$$

and the ramp perturbation in 0.2 second which follows [19]

$$a_2(t) = \begin{cases} a_2(0)(1 - 0.11667t), & t < 0.2 \\ a_2(0)(0.97666), & t \geq 0.2 \end{cases} \quad (22)$$

These transients were simulated by using the proposed ACNEM for 0.5 seconds by the time step length of 0.01 seconds for both perturbations. Thus the

Table 8. Static results for TWIGL SEED-BLANKET-2-D reactor problem

	k _{eff} ^a	k _{eff} relative error [%]	Maximal power relative error [%]	Average power relative error [%]
ACNEM	0.91276	-0.046	4.69	1.68

^a k_{eff}(reference): 0.91318

dynamic calculation was carried out for 50 time steps. According to Christensen [19], the reference for both transkeff Relative Error %ients is the results of the QUANDRY code.

After exerting the step perturbation in region 1 of the reactor core, in respect to eq. (21), results were obtained step by step during the time. Relative average powers in the reactor vs. time dedicated to the time-dependent ACNEM, are compared with the reference in tab. 9. Moreover, values of relative average power calculated by the developed simulator and the reference against the time are illustrated in fig. 5.

For ramp perturbation, the transient was modeled during the time according to eq. (22). Achieved relative average powers and theirs relative errors as for the reference are presented in tab. 10 for some times. In addition, calculated relative average powers and the reference vs. the time for ramp perturbation are shown in fig. 6.

Relative errors of powers given in tabs. 9 and 10 show that the proposed approach has an efficient performance in time-dependent modeling of perturbations. Furthermore, from figs. 5 and 6, one can see the different forms of power enhancement vs. time. This case comes from the variant natures of implemented perturbations.

Table 9. Relative average power vs. time for step perturbation of TWIGLSEED-BLANKET-2-D reactor problem

Time [s]	ACNEM ^a	Reference	Relative error [%]
0.00	1.000	1.000	–
0.05	2.008	–	–
0.10	2.050	2.061	-0.549
0.15	2.059	–	–
0.20	2.068	2.078	-0.489
0.25	2.076	–	–
0.30	2.085	2.095	-0.479
0.35	2.094	–	–
0.40	2.102	2.113	-0.510
0.45	2.109	–	–
0.50	2.120	2.131	-0.533

^a Time step length: 10⁻² s

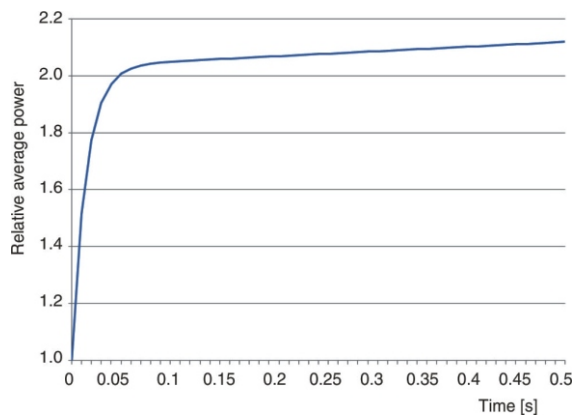


Figure 5. Relative average power vs. time for the step perturbation of TWIGL seed-blanket reactor

Table 10. Relative average power vs. time for ramp perturbation of TWIGL SEED-BLANKET-2-D reactor problem

Time [s]	ACNEM ^a	Reference	Relative error [%]
0.00	1.000	1.000	–
0.05	1.124	–	–
0.10	1.307	1.307	0.019
0.15	1.565	–	–
0.20	1.955	1.957	-0.107
0.25	2.054	–	–
0.30	2.065	2.074	-0.412
0.35	2.074	–	–
0.40	2.083	2.09	-0.446
0.45	2.091	–	–
0.50	2.100	2.109	-0.430

^a Time step length: 10⁻² s

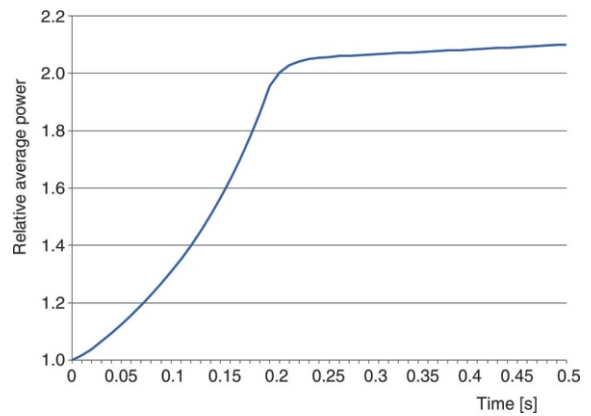


Figure 6. Relative average power vs. time for the ramp perturbation of TWIGL seed-blanket reactor

In the step transient, the power increase quickly occurred during the small time distance *i. e.* $0 < t < 0.05$, similar to the prompt jump response which occurs due to inducing a step reactivity in the system. Also, the nearly linear enhancement of power is seen in fig. 6 for the ramp transient due to the linear decrease of the thermal absorption cross section during $0 < t < 0.2$. Therefore, these cases can prove the proper effect of developed kinetics simulator for this problem.

Problem 3: LMW LWR-3-D

As the third test case, a 3-D reactor core called the LMW (Langenbuch-Maurer-Warner) problem was modeled. This reactor has a two-zone core containing 77 fuel assemblies with widths of 20 cm. The core is reflected by 20 cm of water both radially and axially, and the height of the active core is 160 cm. Radial and axial views of the core for LMW LWR-3-D are indicated in figs. 7 and 8, respectively. In addition, the neutronic parameters and also constants for delayed neutrons belonged to LMW LWR-3-D are given in tabs. 11 and 12, respectively [7]. The defined transient for this problem is the movement of two groups

Figure 7. Quadrant of LMW LWR-3-D in the radial direction

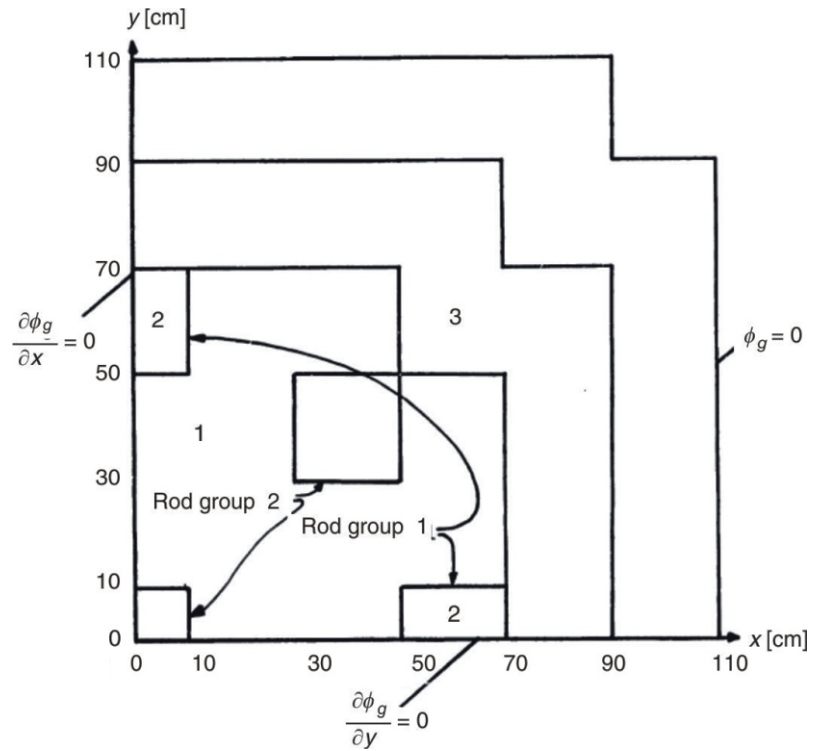


Figure 8. Quadrant of LMW LWR-3-D in the axial direction

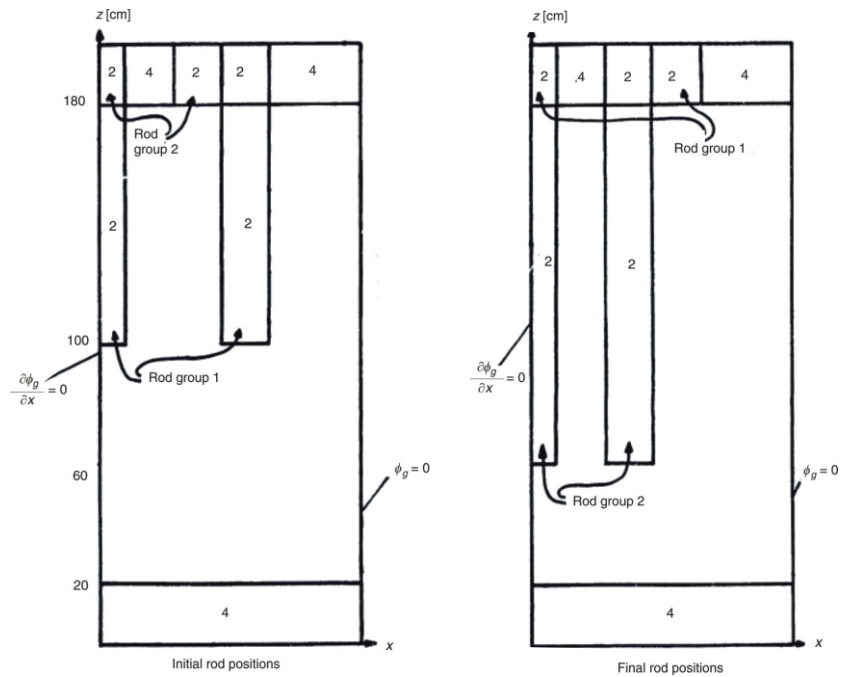


Table 11. Cross-sections of LMW LWR-3-D problem

Region	Group, g	D_g [cm]	Σ_{ag} [cm ⁻¹]	$\nu\Sigma_{fg}$ [cm ⁻¹]	$\Sigma_{1 \rightarrow 2}$ [cm ⁻¹]
1	1	1.423913	0.01040206	0.006477691	0.0175555
	2	0.356306	0.08766217	0.1127328	
2	1	1.423913	0.01095206	0.006477691	0.0175555
	2	0.356306	0.08766217	0.1127328	
3	1	1.425611	0.01099263	0.007503284	0.01717768
	2	0.350574	0.09925634	0.1378004	
4	1	1.634227	0.002660573	0.0	0.02759693
	2	0.264002	0.04936351	0.0	

$\nu_1 = 1.25 \cdot 10^7 \text{ cms}^{-1}$, $\nu_2 = 2.5 \cdot 10^5 \text{ cms}^{-1}$

Table 12. Parameters of delayed neutrons for the LMW LWR-3-D

Parameter	$d = 1$	$d = 2$	$d = 3$	$d = 4$	$d = 5$	$d = 6$
β_d	0.000247	0.0013845	0.001222	0.0026455	0.000832	0.000169
λ_d	0.0127	0.0317	0.115	0.311	1.40	3.87

control rods in which the initial and final positions of them are specified in fig. 8.

For the steady-state calculation, the control rod group 1 was located in the initial position as shown in fig. 8. The static solution was fulfilled by using the developed ACNEM for the quarter symmetry of LMW LWR-3-D. The modeling was performed by utilizing coarse meshes having sizes of the FA, *i. e.* the width of 20 cm in all of the 3-D. Moreover, the reference solution is the results of QUANDRY code [7]. Static parameters containing the effective multiplication factor and its relative error, the maximum and average of power errors for fuel assemblies in comparison to the reference are presented in tab. 13. According to the results, a good agreement between the calculated results and the reference can be observed.

For the time-dependent calculation, a perturbation program is implemented as follows [7]

$$\begin{aligned} &\text{Removing rod group 1 at } 3.0 \text{ cms}^{-1}; 0 \quad 1 \quad 26.666\text{s} \\ &\text{Inserting rod group 2 at } 3.0 \text{ cms}^{-1}; 7.5 \quad 1 \quad 47.5\text{s} \end{aligned} \quad (23)$$

According to fig. 2, the transient solution was accomplished for 60 seconds step by step with the time

Table 13. Static results for LMW LWR-3-D reactor problem

ACNEM	k_{eff}^a	k_{eff} relative error [%]	Maximal power relative error [%]	Average power relative error [%]
	1.00058	0.091	4.02	1.65

^a k_{eff} (reference): 0.99966

Table 14. Relative average power versus time for LMW LWR-3-D problem

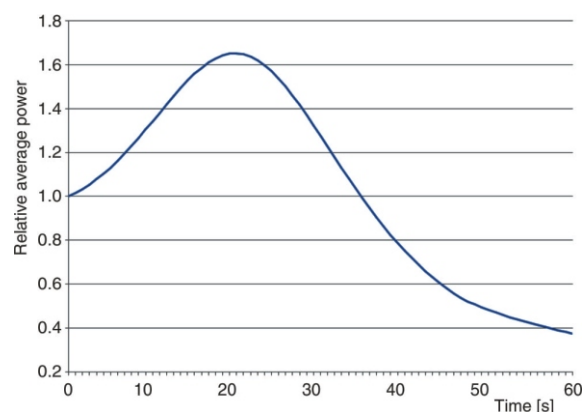
Time [s]	ACNEM ^a	Reference	Relative error [%]
0	1.000	1.000	–
5	1.131	1.114	1.53
10	1.341	1.313	2.16
15	1.559	–	–
20	1.652	1.669	–1.03
25	1.537	–	–
30	1.275	1.340	–4.89
35	0.990	–	–
40	0.752	0.793	–5.11
45	0.580	–	–
50	0.482	0.494	–2.36
55	0.421	–	–
60	0.374	0.379	–1.23

^a Time step length: 0.8 s

step length of 0.8 seconds. For this purpose, the time-dependent two-energy group neutron diffusion equations coupled with six groups delayed neutron equations were solved by launching corresponding changes of cross-sections according to the program of control rods movements noted in eq. (23). Obtained relative average powers in the core for some time steps were compared with the reference [7], in tab. 14. As displayed in tab. 14, a suitable accuracy of developed time-dependent ACNEM is distinguished relative to the reference. Consequently, according to the results, the proposed approach can be reliable for careful simulating of the transient sketches in nuclear reactors. In respect to eq. (23), the schematic diagrams of relative average power changes gained by the applied method and the reference against time are also depicted in fig. 9.

CONCLUSION AND OUTLOOK

The aim of this work was to develop a 3-D time-dependent simulator for solving transient problems of nuclear reactor cores based on the average current nodal expansion method (ACNEM). For this purpose, an adapted iterative algorithm was proposed for solving coupled time-dependent neutron diffusion equations. In this iterative strategy, an inner iteration was considered based on the novel algorithm used in the steady-state treatment. Three transient test cases were simulated by using coarse meshes of sizes of FA for validating the developed approach. Numerical results of both static and dynamic calculations using the time-dependent ACNEM were compared and benchmarked with reported results in references. According to the re-

**Figure 9. Relative average power versus time for the LMW LWR-3-D**

sults, the developed simulator can accurately solve transient problems in a nuclear reactor's core. Furthermore, it was found that when using the developed iteration algorithm, no divergence appeared neither in static nor in transient calculations.

AUTHORS CONTRIBUTIONS

The calculations were done and checked by all the authors. Also, all the authors participated in the preparation of the final version of the manuscript.

REFERENCES

- [1] Caron, D., et al., New Aspects in the Implementation of the Quasi-Static Method for the Solution of Neutron Diffusion Problems in the Framework of a Nodal Method, *Ann. Nucl. Energy*, 87 (2016), 1, pp. 34-48
- [2] Pazirandeh, A., et al., Development of a Computer Code for Neutronic Calculations of a Hexagonal Lattice of Nuclear Reactor Using the Flux Expansion Nodal Method, *Nucl Technol Radiat*, 28 (2013), 3, pp. 237-246
- [3] Koreshi, Z., et al., Variational Methods and Speed up of Monte Carlo Perturbation Computations for Optimal Design in Nuclear Systems, *Nucl Technol Radiat*, 34 (2019), 3, pp. 211-221
- [4] Jahanfarnia, Gh., et al., Neutronic Simulation of a CANDU-6 Reactor with Heavy Water-Based Nano-fluid Coolant, *Nucl Technol Radiat*, 32 (2017), 4, pp. 320-326
- [5] Yasinsky, J. B., Henry, A. F., Some Numerical Experiments Concerning Space-Time Reactor Kinetics Behavior, *Nucl. Sci. Eng.*, 22 (1965), 2, pp. 171-181
- [6] Grossman, L. M., Hennart, J. P., Nodal Diffusion Methods for Space-Time Neutron Kinetics, *Prog. in Nuc. Energy*, 49 (2007), 3, pp. 181-216
- [7] Smith, K. S., An Analytic Nodal Method for Solving The Two-Group, Multidimensional, Static and Transient Neutron Diffusion Equations, Submitted in Partial Fulfillment of The Requirements for The Degrees of Nuclear Engineer and Master of Science at The Massachusetts Institute of Technology, Boston, Mass., USA, 1979
- [8] Putney, J. M., Nodal Methods for Solving the Diffusion Equation for Fast Reactor Analysis, Ph. D. Thesis. University of London, London, UK, 1984
- [9] Poursalehi, N., et al., Performance Comparison of Zeroth Order Nodal Expansion Methods in 3-D Rectangular Geometry, *Nucl. Eng. Des*, (2012), pp. 248-266
- [10] Poursalehi, N., et al., Three-Dimensional High Order Nodal Code, ACNECH, for the Neutronic Modeling of Hexagonal-Z Geometry, *Ann. Nucl. Energy*, 68 (2014), pp. 172-182
- [11] Ginestar, D., et al., High Order Backward Discretization of the Neutron Diffusion Equation, *Ann. Nucl. Energy*, 25 (1998), pp. 47-64
- [12] Pintor, S. G., et al., Preconditioning the Solution of the Time-Dependent Neutron Diffusion Equation by Recycling Krylov Subspaces, *Int. J. Comput. Math*, 91 (2014), pp. 42-52
- [13] Miro, R., et al., A Nodal Modal Method for the Neutron Diffusion Equation Application to BWR Instabilities Analysis, *Ann. Nucl. Energy*, 29 (2002), pp. 1171-1194
- [14] Dulla, S., et al., The Quasi-Static Method Revisited, *Prog. Nucl. Energy*, 50 (2008), 8, pp. 908-920
- [15] Ferrandiz, A. V., et al., Moving Meshes to Solve the Time-Dependent Neutron Diffusion Equation in Hexagonal Geometry, *J. Comput. Appl. Math.*, 291 (2016), Jan., pp. 197-208
- [16] Poursalehi, N., et al., Development of a High Order and Multi-Dimensional Nodal Code, ACNEC3D, for reactor Core Analysis, *Ann. Nucl. Eng.*, 55 (2013), pp. 211-224
- [17] Finnemann, H., et al., Interface Current Techniques for Multidimensional Reactor Calculations, *Atomkernenergie*, 30 (1977), 2, pp. 123-128
- [18] Stacey, M. W., *Nuclear Reactor Physics*, 2th ed. John Wiley & Sons, Weinheim, Germany, 2007
- [19] Christensen, B., Three-Dimensional Static and Dynamic Reactor Calculations by The Nodal Expansion Method, Ph. D. Thesis, Riso National Laboratory, DK-400 Roskilde, Denmark, 1985
- [20] ***, Argonne Code Center, Numerical Determination of the Space, Time, Angle, or Energy Distribution of Particles in an Assembly. Benchmark Problem Book, Argonne National Laboratory, 7416, 1977
- [21] Hageman, L. A., Yasinsky, J. B., Comparison of Alternating Direction Time- Differencing Methods and other Implicit Methods for the solution of the Neutron Group Diffusion Equations, *Nucl. Sci. Eng.*, 38 (1969), 1, pp. 8-32, (published online 13 May 2017)

Received on January 21, 2020

Accepted on September 21, 2020

Камбиз ВАЛАВИ, Али ПАЗИРАНДЕХ, Голамреза ЈАХАНФАРНИЈА

**ТРОДИМЕНЗИОНАЛНА ВРЕМЕНСКИ ЗАВИСНА СИМУЛАЦИЈА
НЕУТРОНСКЕ ДИФУЗИЈЕ ПРИМЕНОМ НОДАЛНЕ МЕТОДЕ СА
РАЗВОЈЕМ СРЕДЊЕ СТРУЈЕ НЕУТРОНА У РЕД**

За временски зависну неутронску симулацију прелазних појава у језгру нуклеарног реактора развијена је нодална метода са развојем средње струје неутрона у ред. У ту сврху, усвојен је итеративни алгоритам за решавање тродимензионалне временски зависне једначине дифузије неутрона. По овој нодалној методи, област језгра реактора може се моделовати грубим мрежама за неутронски прорачун повезан са умереном прецизношћу резултата. Према имплицитној диференцијалној шеми, у временски зависним једначинама извршена је дискретизација чланова диференцијалних по времену. Предложена стратегија примењена је у неким кинетичким проблемима, укључујући реактор у виду бесконачне плоче, дводимензионални TWIGL реактор са прекривачем и тродимензионални LMW LWR реактор. Најпре је одређено решење у стационарном стању за сваки тест случај, а затим је извршен динамички неутронски прорачун током одређеног времена за специфични сценарио прелазног стања. Добијени резултати статичких и динамичких решења верификовани су поређењем са познатим референтним вредностима. Резултати указују на могућност развијеног поступка прорачуна да симулира прелазне појаве у језгру нуклеарног реактора.

Кључне речи: нодална метода, струја неутрона, груба мрежа, дифузиона једначина, правоугаона геометрија, временски зависан прорачун, симулација прелазних стања
